IEEE Access
Multidisciplinary | Rapid Review | Open Access Journal

Received November 17, 2019, accepted December 5, 2019, date of publication December 10, 2019,
date of current version December 23, 2019.

Digital Object Identifier 10.1109/ACCESS.2019.2958853

Design and Fabrication of a Thick Film Heat Flux Sensor for Ultra-High Temperature Environment

TONG ZHANG, QIULIN TAN, (Senior Member, IEEE), WEN LYU, XIAO LU, AND JIJUN XIONG

Key Laboratory of Instrumentation Science and Dynamic Measurement, Ministry of Education, North University of China, Taiyuan 030051, China
Science and Technology on Electronic Test and Measurement Laboratory, North University of China, Taiyuan 030051, China

Corresponding author: Qiulin Tan (tanqiulin@nuc.edu.cn)

This work was supported in part by the National Natural Science Foundation of China under Grant U1837209, Grant 51425505, and Grant 61471324, in part by the Outstanding Young Talents Support Plan of Shanxi province, and in part by the Shanxi ''1331 Project'' Key Subjects Construction.

ABSTRACT In this paper, a ceramic-based thick film heat flux sensor (TFHFS) to monitor the heat flux in high-temperature environments is described. The TFHFS consists of 130 pairs of Pt-Pt/Rh thermocouples distributed in a serpentine form on a ceramic substrate. An insulator was used to generate the temperature difference, which increases the thermoelectric potential (output voltage) and improves the sensitivity of the proposed TFHFS. There are two pairs of independent thermocouples for temperature monitoring. The screen-printing process is used as the fabrication process. The characterization results indicate that the Pt electrodes and the Pt/Rh electrodes were well connected after sintering at 1350°C, and the thickness and width of the thermocouple electrodes were approximately 20 μm and 300 μm, respectively. The test results indicate that the proposed heat flux sensor has a maximum output voltage of approximately 1.44 mV, and the heat flux sensitivities for 3–57 kW/m^{2}were well distributed in the range of 0.025–0.030 mV/(kW/m^2), thereby demonstrating that the fabricated sensor exhibits high sensitivities in the given heat flux range. Furthermore, the reusability investigation indicated that the prepared TFHFS achieves a stable output voltage and a low error level at 50–900 °C. Therefore, we assume that the proposed sensor can be used for monitoring the heat flux in harsh applications such as turbomachinery and aerospace industries.

INDEX TERMS Ceramic sensor, heat flux sensor, high temperature monitoring, thermocouple.

I. INTRODUCTION

Heat flux measurement for thermal energy transfer research is indispensable in harsh environments, such as nuclear plants and modern turbomachinery, or searing temperatures, high heating rates, and aerodynamic loads in a spacecraft thermal protection system [1]–[3]. A good heat flux sensor should have the advantages of small size, least interference with the environment, high accuracy, and sensitivity [4]. Moreover, long term measurement of heat flux in the applications mentioned is highly required. For example, as fuel costs increase, airlines face a challenge to reduce fuel consumption, and the next-generation commercial aircraft will be required to have a higher fuel efficiency. The easiest way to achieve this is to run the engine at higher temperatures. Therefore, there is an urgent need for a heat flux sensor capable of withstanding higher temperatures to achieve heat flux monitoring in a high-temperature environment, to control heat transfer efficacy [5].

Several heat flux sensors such as the thin film type, Gordon type, and plug type sensors have been developed [6]–[12]. Scott D. Wilson studied a thin film heat flux sensor array, which is used for heat flux testing in the Stirling Convertor. This gauge requires a complex cold end compensation, and owing to its thickness, it exhibits a slow response to the heat flux [7]. Christopher reported a thin film heat flux sensor that consisted of a series of Pt/Rh thermocouples based on different substrates. Despite its high response frequency (3 kHz), it exhibited low sensitivity [13]. Theophilos S and his team developed a heat flux sensor, using thermal spraying technology, and realized heat flux test at 100 °C [14]. Wilson S D designed a thin film resistance heat flux sensor and measured the heat flux at 120 °C. However, a high-temperature test was not conducted in this study [6]. A majority of heat flux sensors employed in high-temperature environments require the use of water-cooled devices, such as the Schmidt-Boelter

The associate editor coordinating the review of this manuscript and approving it for publication was Yassine Maleh.

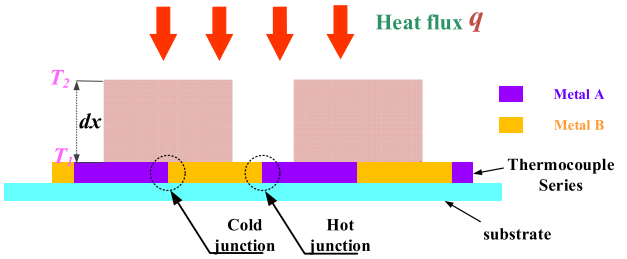

FIGURE 1. The theory of heat flux measurement in this design.

and Gordon models), resulting in cumbersome measurement systems [15]. Therefore, it is necessary to develop a high-temperature heat flux sensor that does not require water cooling. Moreover, the fabrication process of the heat flux sensors mentioned above are complicated and expensive. Thick film sensors have the same advantages as thin film sensors, such as lower impact on the test environment and shorter response times [13], [16]. More importantly, the thickness of the thick film sensors is 10 times or more than that of thin film sensors; hence, thick film sensors have better durability at ultra-high temperatures and are more suitable for use in harsh environments.

In this study, a thick film heat flux sensor (TFHFS) based on one-dimensional heat transfer was investigated. This sensor is based on Al_2O_3 ceramic and there are 130 pairs of Pt-Pt/Rh thermocouples distributed on it in a serpentine fashion. Screen-printing is used for depositing the thermocouples and realizing thermocouples conjunctions. Platinum (Pt) and platinum/10% rhodium (Pt/Rh) are selected as the thermoelectric material. The morphological and parameters characteristics of this sensor was investigated via a laser confocal microscope and scanning electron microscope (SEM). Eventually, the sensing performance of as the fabricated sensor was analyzed. Compared with the heat flux sensors [17] designed previously, this design integrates more thermocouples within the same area and simplifies the manufacturing process. Furthermore, the installation and test direction of the sensors are changed to reduce the influence of the substrate heat conduction on the test results of the sensor. In addition, two pairs of independent thermocouples are added for temperature monitoring.

A. PRINCIPLE

The heat flux sensor is based on Fourier's Law and Seebeck effect. The theory of heat flux measurement in this design is shown in Fig. 1.

According to Fourier's Law, the calculation formula of heat flux density q is shown in (1).

$$q = kdT/dx \tag{1}$$

q represents the heat flux flowing across the interface, k is the thermal conductivity of object, while dT/dx is the variable rate of temperature difference across the thickness of designated object. According to the Seebeck effect, the thermocouple

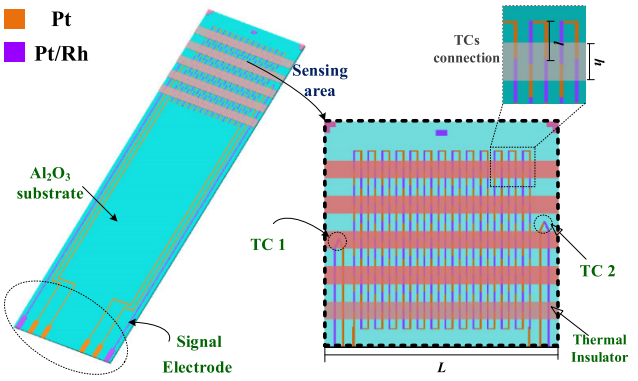

FIGURE 2. Structural diagram of the designed TFHFS.

series positioned in parallel has an output voltage U as:

$$U = NS_{AB}dT \tag{2}$$

N is the amount of thermocouple (TC), and S_{AB} represents the Seebeck coefficient of TC metal (metal A and B, shown in Fig. 1).

Sensitivity S of heat flux sensor is defined as:

$$S = U/q \tag{3}$$

By synthesizing (1), (2), and (3), S equals to:

$$S = NS_{AB}dx/k \tag{4}$$

Therefore, from (4), the sensitivity S is related to N, k, dx and the Seebeck coefficients of TC materials. Moreover, as shown in (2), the output voltage is dependent on N, dT, and the Seebeck coefficients of TC materials.

B. SENSOR DESIGN

Based on the mechanism analysis, a TFHFS for harsh environments was proposed, as shown in Fig. 2. To enhance the durability of the sensor in high-temperature environments, the sensor was based on an Al_2O_3 ceramic substrate, while platinum (Pt) and platinum/10% rhodium (Pt/Rh) were designated as the TC materials. The TCs were connected in a serpentine form and located on the surface of the alumina ceramic substrate being used as the sensing space. Nano-structured silicon oxide has a thermal conductivity of 0.013 w/m/k and acts as a thermal insulator. It covers half of the TC, as shown in Fig. 2. In addition, two separate pairs of thermocouples are located on either side of the thermocouple series for temperature monitoring. The hot junction of one thermocouple (TC1) is buried under the thermal insulation layer to measure the temperature under insulation, and the other thermocouple (TC2) is directly exposed to the air to measure ambient temperature.

The Pt and Pt/Rh signal electrodes, as shown in Fig. 2, are extended from the high-temperature region to the low-temperature region, which is conducive to the readout of the test signal. The thermoelectric potentials of the 130 pairs of thermocouples, owing to the temperature difference between

TABLE 1. Parameters of TFHFS.

Parameters	L	h	l	T_i	T_c	T_t	d
Value	40 mm	3 mm	3.4 mm	130 μm	635 μm	20 μm	300 μm

TABLE 2. Parameters of screen-printing mesh.

Parameters	Mesh size	Film thickness	Angle	Screen force	Line width
Value	200 mesh/inch	20 μm	22.5°	29N	40 μm

the hot and cold junctions, is connected in series to obtain the output voltage of the heat flux sensor. Table 1 lists the associated parameters of the designed TFHFS. Note that h is the width of insulator; L is the side length of sensing area, which is a square; T_x represents the thickness, where x denotes insulator, ceramic substrate, or thermocouple; l and d are the length and width of Pt or Pt/Rh electrode of single TC, respectively.

II. SENSOR FABRICATION

A. FABRICATION

The combination of screen-printing technology and ceramic electronic manufacturing is simpler and cheaper than other methods [18], and it has been proven to be an effective and controllable fine electrode forming technology in our previous work. Based on this, screen-printing technology was employed as the method to fabricate the proposed TFHFS. The parameters of the screen-printing mesh are presented in Table 2.

As illustrated in Fig. 3, the roughness at the surface of the Al_2O_3 chip was first polished to 0.4 μm, which was beneficial for the bonding between the thermocouple metal and the ceramic chip. Then, the ceramic substrate was washed with an anhydrous ethanol solvent to remove impurities. After that, 5599-P type Pt conductors were screen-printed onto the ceramic substrate and dried at 100 °C for 20 min to solidify and shape the Pt electrodes of TCs and the Pt signal electrode. To locate and connect the Pt electrodes fabricated in the initial screen-printing process, the mesh was aligned through labels on the substrate. The mesh and screen-printing processes were repeated using 5799-X type Pt/Rh conductor paste (ESL Electronic Company, USA) to form the Pt/Rh electrodes of the TC on the surface of the substrate.

Similarly, the Pt/Rh electrodes just printed were dried in the same conditions as the Pt electrodes shaping process for solidifying and shaping the Pt/Rh electrodes. Eventually, screen-printed TFHFS was fired in muffle furnace according to the sintering curve shown in Fig. 4.

In stage 1 of the temperature, the solvents of the conductor evaporated and the conductor dried, and in stages 2 and 3, the stable bonding between the substrate and the TCs was built, and the Pt electrodes and the Pt/Rh electrodes were welded together. As the temperature exceeded 1350 °C, it was maintained for 30 min and then cooled to room temperature,

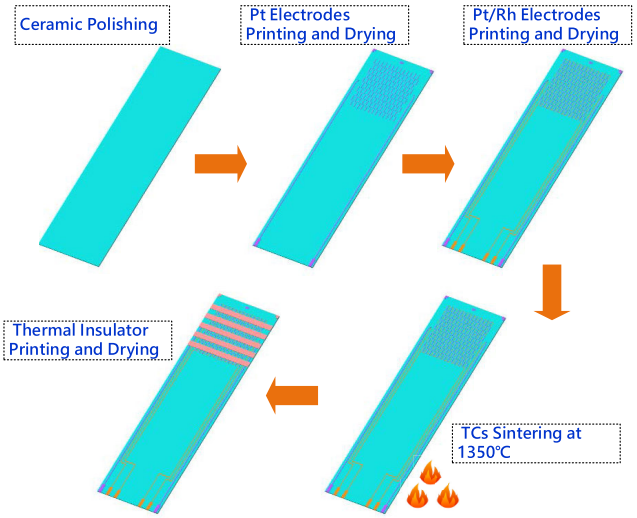

FIGURE 3. Process of fabricating the designed heat flux sensor.

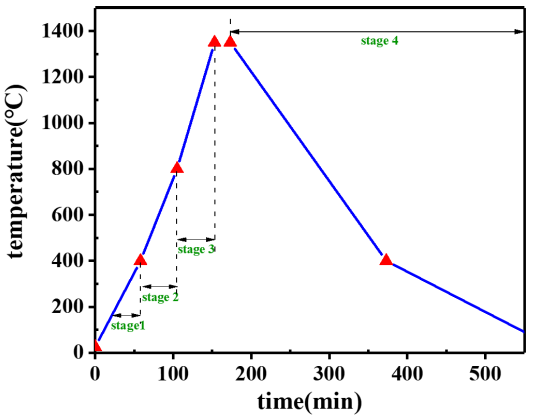

FIGURE 4. Sintering curve of the proposed heat flux sensor (stage 1: the solvents of the conductor evaporating and the conductor drying; stages 2 and 3: building the stable bonding between the substrate and the TCs, and welding the Pt electrodes and the Pt/Rh electrodes; stage 4: cooling).

in stage 4. A nano-structure silicon oxide insulator was coated on the ceramic substrate via a mask, and the insulator was dried at 70 °C. The mask is a self-made green tape (an LTCC chip before firing at high temperature) with five rectangular holes. The location and size of the rectangular holes are determined by the size of the insulation layer. The preparation process of the insulation layer is as follows: first, the mask is covered on the alumina substrate, then, the rectangular holes of the mask are covered with the prepared silica solution. After the silicon dioxide solidifies, the mask is removed, and the silicon dioxide solidifies on the substrate to form the insulator layer. Fig. 5 shows the TFHFS before and after coating with the insulator. The hot junction of TC1 is covered with insulation and TC2 is directly exposed to the measurement environment.

B. CHARACTERISATION

By dint of Laser Confocal Microscope, we characterized the fabricated TFHFS and the corresponding result was shown

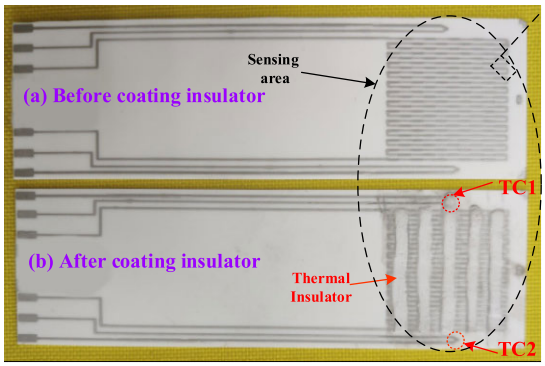

FIGURE 5. TFHFS before and after coating with the insulator.

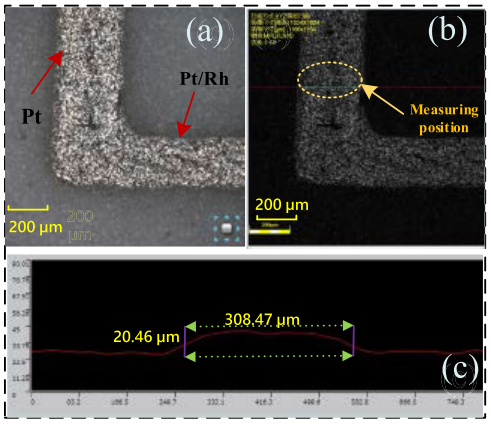

FIGURE 6. (a), (b) Scanning relief image of a Pt-Pt/Rh conjunction under different microscope modes; (c) thickness and width characterization result of Pt electrodes in (a).

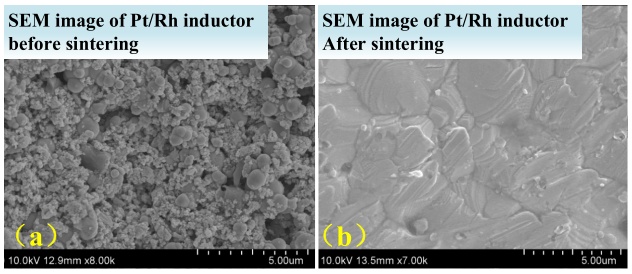

FIGURE 7. (a) SEM image of Pt/Rh inductor before sintering; (b) SEM image of Pt/Rh inductor after sintering.

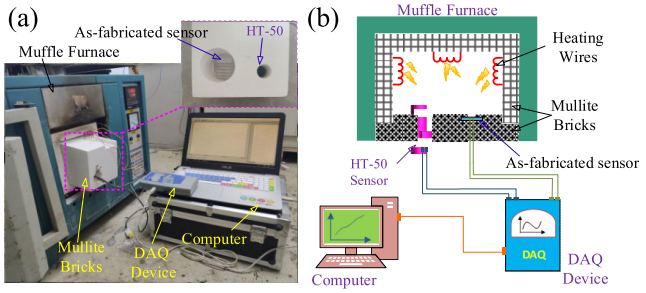

FIGURE 8. (a) The test system used for TFHFS performance (the inset is the installation of calibration sensor and the prepared heat flux sensor in the wall of muffle furnace); (b) the schematic of the test platform corresponding to (a).

in Fig. 6. Fig. 6 (a) is an image of Pt-Pt/Rh conjunction observed by the laser confocal microscope. As shown in Fig. 6 (a), the Pt electrode and the Pt/Rh electrode are well connected after sintering. We measured the thickness and width of the Pt electrode in Fig. 6 (a), the horizontal line in Fig. 6 (b) marks the specific location of the measurement. The measurement result is shown in Fig. 6(c). The width and thickness of this Pt electrode are approximately 300 μm and 20 μm, respectively, which are consistent with the screen parameters.

On visual inspection, it was observed that, with the increase in the sintering temperature, the sintered film gradually changed from gray black to silver gray and finally to bright white with a metallic luster at 1350 °C. The SEM images of the metal films were obtained by field emission scanning electron microscopy (FEI Quanta, 250 FEG). As Pt and Pt/Rh have similar structures and lattice constants, their SEM images are very similar. We mainly analyzed the microstructure of the Pt/Rh films. Fig. 7 (a) and (d) present the microstructures of the Pt/Rh films before and after sintering, respectively. It can be seen from the figure that after high-temperature sintering, the binder in the metal slurry volatilizes, and the metal film changes from loose platinum powder to dense sinter. It is also found that the sensitive film is not conductive before sintering and has a good conductivity after sintering. In view of these results, we believe that the preparation process is effective for the preparation of the proposed heat flux sensor.

III. TFHFS PERFORMANCE EVALUATION

The test platform, as shown in Fig. 8 (a), is built to test the prepared sensor, and Fig. 8 (b) is the schematic diagram of the test platform. Muffle furnace is used to provide the high temperature and heat flux environment. The HT-50 multi-sensor (ITI, USA) for heat flux calibration and temperature measurement is fixed on the same mullite brick with the fabricated sensor. The sensitive surfaces of the two sensors are parallel and perpendicular to the heat flux direction.

The DAQ device (Fourtec, Israel) was used for transferring and processing the heat flux signal and output voltage to a computer where the they were displayed. In the furnace, the inner space was sealed with mullite bricks and heating wires were distributed evenly in the wall.

A series of performance tests of TFHFS were carried out in the air of 50-900 °C in muffle furnace. The heating speed of muffle furnace is 3 °C /min and 10 °C /min respectively in the range of 50-300 °C and 300-900 °C, which is set according to the use requirements of muffle furnace. After a long period of repeated tests, the test results are shown in Fig. 9 and Fig. 10.

Figure 9 shows the T-q curve measured by the HT-50 sensor. T, q are the temperature and heat flux, respectively, measured by the HT-50 standard sensor as the temperature changes in the furnace. In this case, the sensor surface

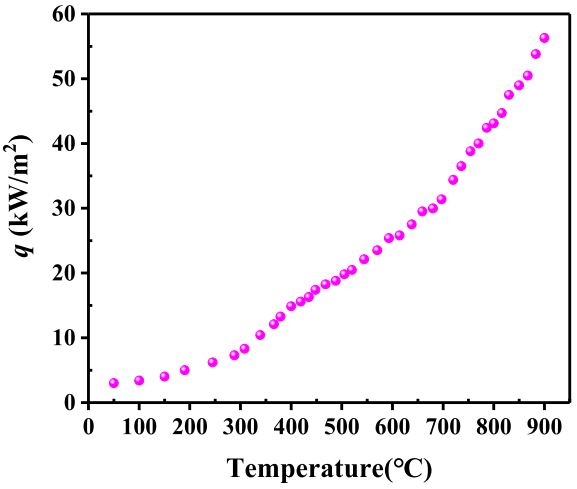

FIGURE 9. Heat flux versus temperature curve of HT-50 calibration sensor tested at 50-900 °C.

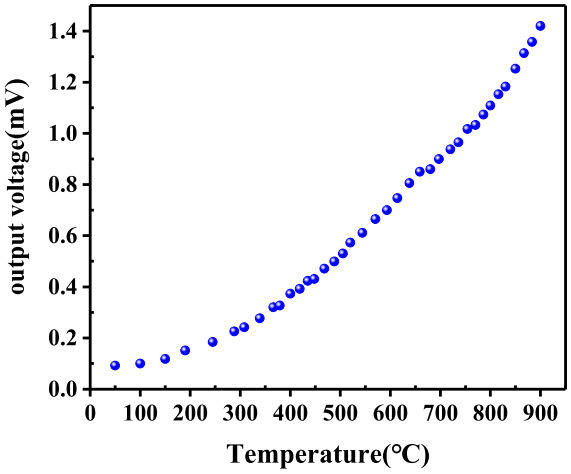

FIGURE 10. Output voltage versus temperature curve of TFHFS tested at 50-900 °C.

temperature rises from 50 °C to 900 °C, and the heat flux measured by the standard HT-50 sensor is about 3-57kW/m^2. The result implied that the heat flux generated in the furnace increases continually as the temperature ramps up. We also observed that, compared with other temperature ranges, the heat flux measured by the HT-50 sensor increased slowly in the range of 50-300 °C. This shows that the growth rate of heat flux is determined by the change rate of temperature in the furnace, which conforms to the definition of heat flux density.

Meanwhile, the T-output voltage curve of the fabricated TFHFS is shown in Fig. 10, the curve of voltage versus temperature of the TFHFS is very consistent with that of the HT-50 sensor. This shows that the sensor can be used to detect the heat flux in the range of 50-900 °C. The maximum output voltage of the sensor is 1.44 mV at 900 °C, which indicates that the sensor has a large output voltage.

In Fig. 11, the output voltage-q curve of TFHFS at 3-57 kW/m^2 is presented, and the result shows that the output

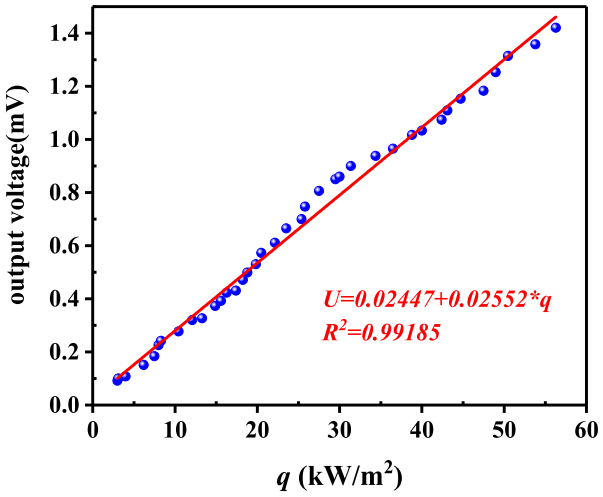

FIGURE 11. Output voltage versus heat flux curve of TFHFS in 3-57 kW/m^2.

voltage of TFHFS improves as the heat flux surges. The fitting result showed that that the output voltage-q curve of TFHFS at 3-57 kW/m^2 matches with a line on a high fitting degree:

$$\mathrm{U} = 0.02447 + 0.02552 * q, \quad \mathrm{R}^2 = 0.99185$$

From the fitting results, the output thermoelectric potential of the heat flux sensor has a good linear relationship with the load heat flux density measured by the standard HT-50 sensor, which is consistent with the theoretical analysis.

The sensitivity of the TFHFS at every heat flux point, calculated by (3), is plotted in Fig. 12. It can be seen that the sensitivities of the fabricated TFHFS in 3-57 kW/m^2 were well distributed in the range of 0.025-0.030mV/(kW/m^2), indicating that the error of sensitivity is approximately 20% in the range of the applied heat flux sensor. In $S = NS_{AB}dx/k$, N and dx have been determined after the sensor is fabricated. However, the Seebeck coefficient of the thermoelectric material and the thermal conductivity k of insulating material are not constant, they will change slightly with the increase of temperature, resulting in the change of the sensor sensitivity S.

The output voltage (U_1, U_2) of the two independent thermocouples (TC1, TC2) versus temperature is shown in Fig. 13. The increasing trend of thermocouple voltage with temperature is the same as that of Pt-Pt/Rh thermocouple in reference [19]. It can be seen from the figure that the output voltage of the two thermocouples in the low temperature section is very small, resulting in a relatively large temperature measurement error below 400 °C. The thermocouple is more suitable for temperature measurement above 400 °C, which is combined with the characteristics of the Pt-Pt/Rh thermocouple. Because the hot junctions of TC1 and TC2 are located in the insulation layer and outside the insulation layer respectively, and the two thermocouples have the same cold-end temperature (T_{cold}). The temperature difference

TABLE 3. The parameters of S_{AB} under different temperatures.

Temperature (°C)	100	200	300	400	500	600	700	800	900
S_{AB} (μV/°C)	7.39	8.46	9.13	9.57	9.9	10.21	10.53	10.87	11.21

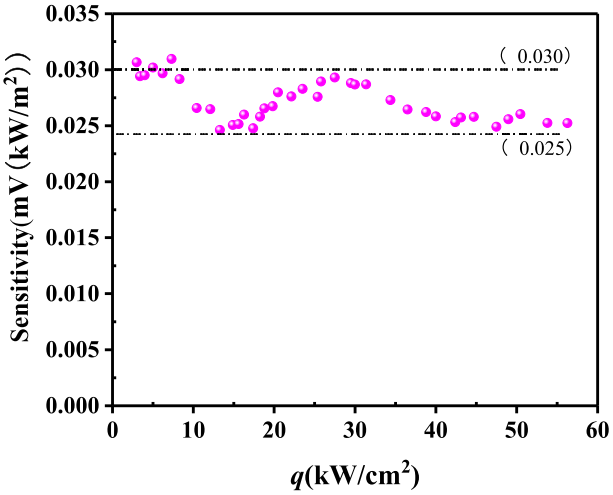

FIGURE 12. Sensitivity versus temperature curve of TFHFS in 3-57 kW/m².

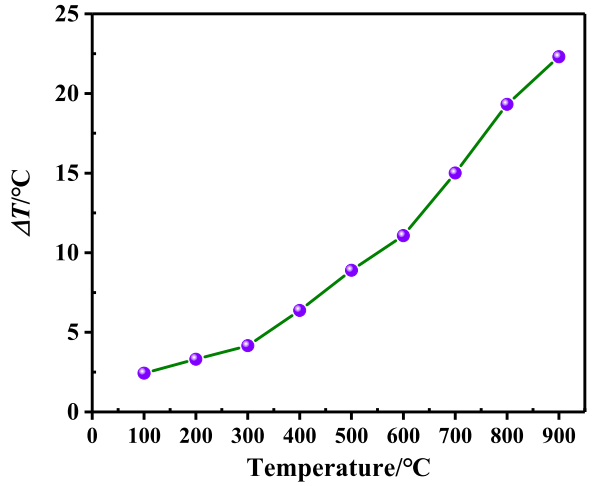

FIGURE 14. Temperature difference of insulation versus temperature curve in 100-900 °C.

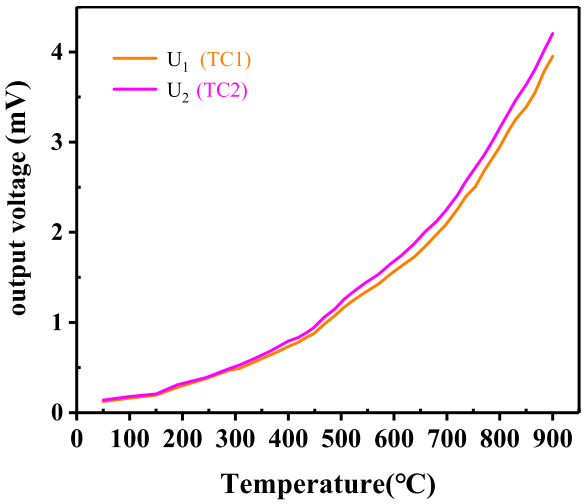

FIGURE 13. Output voltage versus temperature curve of TC1, TC2 at 50-900 °C.

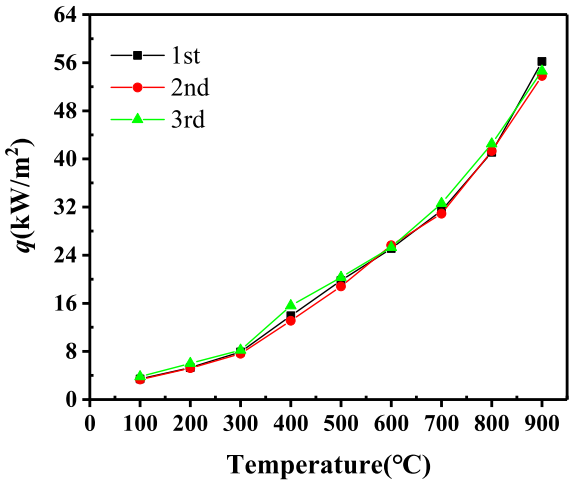

FIGURE 15. The q versus temperature curve of HT-50 calibration sensor in 100-900 °C.

inside and outside the thermal insulator (ΔT) can be calculated.

According to (2),

$$U_1 = NS_{AB} \times (T_{hot1} - T_{cold});$$
$$U_2 = NS_{AB} \times (T_{hot2} - T_{cold});$$
$$\Delta T = T_{hot2} - T_{hot1},$$

Then,

$$\Delta T = (U2 - U1)/(NS_{AB})$$

Moreover, as the Seebeck coefficient of the TCs varies according to Table 3, the calculated results are shown in Fig. 14, indicating that the ΔT at 900 °C was above 22.3 °C. This may be attributed to the huge difference of thermal conductivity between the substrate and the insulator. In addition, TC2 can be used for environmental temperature monitoring because of its hot spot exposed to air directly.

To investigate the reusability of the prepared TFHFS, we tested the sensor three times at 100 - 900 °C and the test results are shown in Fig. 15 and Fig. 16. Fig. 15 demonstrates that the q-T curve at every instance matches well with each

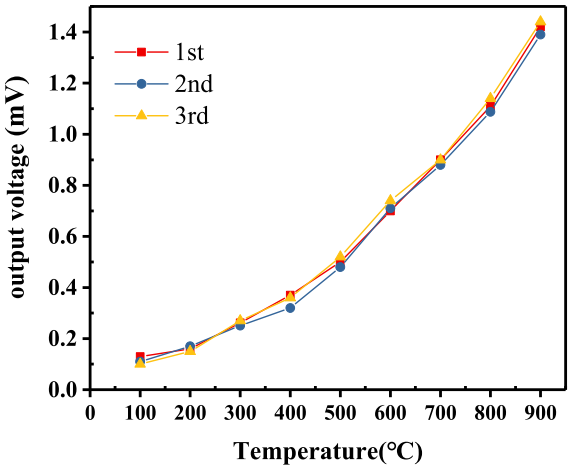

FIGURE 16. The output voltage versus temperature curve of TFHFS in 100-900 °C.

other, and the heat flux generated at 900 °C was 3-57kW/m^2. Moreover, the maximum error of approximately 9.8% can be observed at 400 °C.

Furthermore, the output voltage -T curve of TFHFS in Fig. 16 demonstrates that the output voltage peak of the TFHFS in all the three tests was in the range of 1.39-1.44mV, and all the curves tested under the same conditions show good consistency, indicating that the TFHFS has a stable output voltage in the range of 100–900 °C. The maximum error occurred at 400 °C, and its value is approximately 8.5%. Eventually, by synthesizing the results of Fig. 15 and Fig. 16, we can conclude that the prepared TFHFS shows a good output voltage and stable sensitivity to heat flux at 100-900 °C. In addition, the sensors we manufactured through this process can also work at 1400 °C stably, indicating that the sensors manufactured in this experiment have the potential to work at higher temperatures [20].

IV. CONCLUSION

In this paper, we described a ceramic-based thick film heat flux sensor for high-temperature environments. Screen-printing, which is easy and low-cost, was used for fabricating the TFHFS. The characterization indicated the Pt and Pt/Rh electrodes were well connected after firing at 1350 °C, and the thickness and width of the TCs were approximately 20μm and 300 μm, respectively. The experiments indicated that the designed heat flux sensor has a maximum output voltage of up to 1.44 mV, and the thermal insulation layer can produce a temperature difference of 22 °C at 900 °C. The sensitivities of the fabricated heat flux sensor in 3-57 kW/m^2 were well distributed in the range of 0.025-0.030 mV/(kW/m^2), indicating that the fabricated sensor has a high sensitivity in the given heat flux range. This is attributed to the serpentine integration of numerous thermocouples on the ceramic substrate. Further, the reusability investigation discloses that the prepared TFHFS has a stable output voltage in 100-900 °C with an error of 8.5%. Working at higher temperatures is also possible, but it was not studied here. Therefore, the fabricated sensor can be used for heat flux monitoring in some harsh applications.

REFERENCES

[1] A. H. Epstein, G. R. Guenette, and R. J. G. Norton, "High-frequency response heat-flux gauge," *Rev. Sci. Instrum.*, vol. 57, no. 4, pp. 639–649, 1986.

[2] C. A. Pullins and T. E. Diller, "*In situ* high temperature heat flux sensor calibration," *Int. J. Heat Mass Transf.*, vol. 57, no. 17, pp. 3429–3438, 2010.

[3] A. R. Gifford, D. O. Hubble, and P. A. Clayton, "Durable heat flux sensor for extreme temperature and heat flux environments," *J. Thermophys. Heat Transf.*, vol. 24, no. 1, pp. 69–76, 2010.

[4] R. J. Lubbock, S. Luque, and B. R. Rosic, "A new transient high heat flux convection calibration facility for heat transfer gauges in high enthalpy flows," *J. Heat Transf.*, vol. 140, no. 4, 2017.

[5] J. V. Pearce, G. Machin, and T. Ford, "Optimizing heat treatment of gas turbine blades with a Co-c fixed point for improved in-service thermocouples," *Int. J. Thermophys.*, vol. 29, no. 1, pp. 223–230, 2008.

[6] S. D. Wilson, G. C. Fralick, and J. D. Wrbanek, "Fabrication and testing of a thin-film heat flux sensor for a stirling convertor," *Aiaa J.*, vol. 24, no. 5, pp. 362–369, 2013.

[7] G. Fralick, J. Wrbanek, and C. Blaha, "Thin film heat flux sensor of improved design," in *Proc. 48th Int. Instrum. Symp.*, San Diego, CA, USA, 2002.

[8] R. D. Neumann, "Aerothermodynamic instrumentation," Nasa, Washington, DC, USA, Tech. Rep., 1989.

[9] D. G. Holmberg and T. E. Diller, "High-frequency heat flux sensor calibration and modeling," *J. Fluids Eng.*, vol. 117, no. 4, pp. 659–664, 1995.

[10] J. Kim, T. Kim, and S. Cho, "Modeling and fabrication of thin film thermopile sensor," *J. Vac. Sci. Technol. B*, vol. 27, no. 3, pp. 1466–1472, 2009.

[11] K. B. Sobolik, N. R. Keltner, and J. V. Beck, "Measurement errors for thermocouples attached to thin plates: Application to heat flux measurement devices," in *Proc. ASME/AIChE Nat. Heat Transf. Conf.*, Philadelphia, PA, USA, 1989.

[12] S. A. Raphaelmabel, "Design and calibration of a novel high temperature heat flux sensor," *Asme Summer Heat Transf. Conf. Collocated With Asme Pacific Rim Tech. Conf. & Exhib. Integr. & Packag. MEMS*, 2005, pp. 983–988.

[13] C. S. Cho, G. C. Fralick, and H. D. Bhatt, "Steady-state and frequency response of a thin-film heat flux gauge," *J. Spacecraft Rockets*, vol. 34, no. 6, pp. 793–798, 1997.

[14] T. S. Theophilou, J. P. Longtin, S. Sampath, S. Tankiewicz, and R. J. Gambino, "Integrated heat-flux sensors for harsh environments using thermal-spray technology," *IEEE Sensors J.*, vol. 6, no. 5, pp. 1126–1133, Oct. 2006.

[15] A. V. Mityakov, S. Z. Sapozhnikov, and V. Y. Mityakov, "Gradient heat flux sensors for high temperature environments," *Sens. Actuators A, Phys.*, vol. 176, pp. 1–9, Apr. 2012.

[16] J. F. Lei and H. A. Will "Thin-film thermocouples and strain-gauge technologies for engine applications," *Sens. Actuators A, Phys.*, vol. 65, no. 3, pp. 187–193, 1998.

[17] W. Lyu, Y. Ji, T. Zhang, G. Liu, J. Xiong, and Q. Tan, "A novel ceramic-based heat flux sensor applied for harsh heat flux measurement," in *Proc. IEEE SENSORS*, Oct. 2018, pp. 1–4.

[18] Q. Tan, W. Lyu, and Y. Ji, "A LC wireless passive temperature-pressure-humidity (TPH) sensor integrated on LTCC ceramic for harsh monitoring," *Sens. Actuators B, Chem.*, vol. 270, pp. 433–442, Oct. 2018.

[19] J. V. Pearce, F. Edler, C. J. Elliott, A. Greenen, P. M. Harris, C. G. Izquierdo, Y.-G. Kim, M. J. Martin, I. M. Smith, D. Tucker, and R. I. Veltcheva, "A systematic investigation of the thermoelectric stability of Pt-Rh thermocouples between 1300°C and 1500°C," *Metrologia*, vol. 55, no. 4, p. 558, 2018.

[20] Y. Ji, Q. Tan, and H. Wang, "A novel surface *LC* wireless passive temperature sensor applied in ultra-high temperature measurement," *IEEE Sensors J.*, vol. 19, no. 1, pp. 105–112, Jan. 2019.

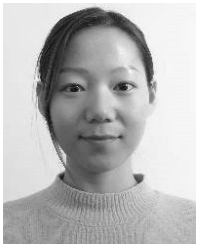

TONG ZHANG received the B.S. degree from the North University of China, Shanxi, China, in 2017, where she is currently pursuing the M.S. degree. Her research interest includes heat flux sensor under harsh environments.

QIULIN TAN received the B.S., M.S., and Ph.D. degrees from the North University of China, Shanxi, China, in 2002, 2006, and 2009, respectively. He has finished studying as a post-doctor in Tsinghua University, in 2015. He is currently a Professor and a Doctoral Supervisor with the North University of China. He has published over 60 articles and one book. His current research interests include nanomaterials, IR gas sensor, wireless passive micro-sensors, smart flexible sensor, and measuring instrument. He received three State/Ministerial prize for progress in science and technology in China.

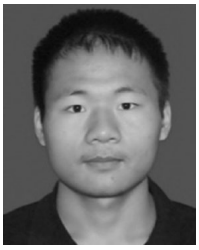

WEN LYU received the B.S. degree in electrical engineering and the M.S. degree from the North University of China, Shanxi, China, in 2016 and 2019. His research interest includes heat flux sensor under harsh environments.

XIAO LU received the B.S. degree from the North University of China, Shanxi, China, in 2015, where she is currently pursuing the M.S. degree. Her research interest includes temperature sensor under harsh environments.

JIJUN XIONG received the B.Sc. and M.Sc. degrees in electrical engineering from the North University of China, Shanxi, China, in 1993 and 1998, respectively, and the Ph.D. degree in precision instruments and technology from Tsinghua University, Beijing, China, in 2003. His research interest is in the fields of measurement and MEMS.